JOURNAL OF VIROLOGY, Oct. 1997, p. 7629–7639 Vol. 71, No. 10
0022-538X/97/$04.00+0

The Cytopathicity of a Simian Immunodeficiency Virus Mne Variant Is Determined by Mutations in Gag and Env

JASON T. KIMATA AND JULIE OVERBAUGH*

Department of Microbiology, University of Washington, Seattle, Washington 98195

Received 11 April 1997/Accepted 18 July 1997

Previous studies suggested that the rapidly replicating, highly cytopathic, syncytium-inducing (rapid-high/SI) phenotype of simian immunodeficiency virus Mne variants that evolved in macaques inoculated with a slowly replicating, minimally cytopathic, non-syncytium-inducing (slow-low/NSI) molecular clone was not solely the result of changes in the envelope surface protein (Env SU). To define the viral determinants responsible for the change in phenotype, we molecularly cloned a rapid-high/SI variant (designated SIVMne170) derived from the peripheral blood mononuclear cells (PBMCs) of a pig-tailed macaque that was inoculated with a slow-low/NSI molecular clone, SIVMneCL8. SIVMne170 was SI and replicated with faster kinetics and was more cytopathic than the parent SIVMneCL8 in CEMx174 cells. Additionally, SIVMne170 was more cytopathic for the CD4$^+$ T-cell population than SIVMneCL8 in macaque PBMCs. An analysis of chimeric viruses constructed between the variant SIVMne170 and the parent virus SIVMneCL8 demonstrated that there are determinants encoded within both the 5′ and 3′ halves of SIVMne170 that independently contribute to its rapid-high/SI phenotype. As we previously observed with other SIVMne variants, the Env SU of SIVMne170 was important for syncytium induction but was not a key determinant of cytopathicity. By contrast, the intracellular domain of the envelope transmembrane protein (Env TM) contributed to both the SI and cytopathic properties of SIVMne170. We also found that the minimal determinant within the 5′ half of SIVMne170 that conferred its rapid replication kinetics and cytopathicity mapped to the capsid- and nucleocapsid-encoding regions of *gag*. Together, these data demonstrate that mutations selected in Gag and Env TM intracytoplasmic tail influence the replication and cytopathicity of SIVMne variants that evolve in the host.

Phenotypic differences are commonly observed between human immunodeficiency virus type 1 (HIV-1) isolates obtained from peripheral blood at early and late stages of infection (30, 32). Viruses isolated early after infection, during the asymptomatic stage, are typically macrophage tropic, slow replicating, minimally cytopathic, and non-syncytium inducing (M-tropic, slow-low/NSI phenotype) (6, 10, 11, 15, 16, 46, 51, 52). Variant viruses that emerge later in infection are frequently able to infect CD4$^+$ T-cell lines and may be rapidly replicating, cytopathic, and syncytium inducing (T-tropic, rapid-high/SI phenotype) (6, 10, 11, 15, 16, 46, 51, 52). While the significance of this shift in phenotype is unclear, the appearance of rapid-high/SI viruses has been associated with high viral loads and rapid CD4$^+$ T-cell decline (reviewed in reference 32). Thus, an understanding of the evolution of rapid-high/SI viruses may provide insight into their role in CD4$^+$ T-cell depletion in the host.

A molecular clone of simian immunodeficiency virus (SIV) Mne (SIVMneCL8) undergoes phenotypic changes during the course of infection in macaques. SIVMneCL8 displays a slow-low/NSI phenotype, and when inoculated into pig-tailed macaques, it evolves into a population of rapid-high/SI viruses in association with the development of AIDS (43). These data suggest that the virological changes that are associated with the decline in CD4$^+$ T cells and progression to AIDS in SIVM neCL8-infected macaques parallel those observed in HIV-1-infected individuals. Importantly, the inoculation of a molecularly cloned virus provides a progenitor of known sequence that can be used to define functional mutations selected during the evolution of the virus over the course of infection. Indeed, previous studies from our laboratory have identified characteristic genetic changes selected in SIVMneCL8 as it evolves in vivo (40, 41, 43). Because this system can distinguish both genetic and phenotypic differences as a cloned slow-low/NSI virus evolves into a population of rapid-high/SI viruses, the specific viral genetic mutations that confer a shift in viral phenotype may be defined by using this model.

Differences in tropism, replication kinetics, and the SI and cytopathic properties of HIV-1 NSI and SI variants have been ascribed to mutations selected in the envelope surface glycoprotein protein (Env SU), gp120 (7, 12, 30). We have also found that mutations selected in Env SU of SIVMne influence the phenotype of the virus, altering antigenicity and SI capacity (4, 44). However, in contrast to the HIV-1 Env SU, the mutations in Env SU of SIVMne do not appear to enhance viral replication or cytopathicity, suggesting that mutations in other viral genes contribute to the evolution of rapid-high/SI variants (44). Thus, to identify the mutations that confer a rapid-high/SI phenotype, we cloned a rapid-high/SI variant that evolved in vivo from the slow-low/NSI pathogenic molecular clone, SIVMneCL8, and examined the phenotype of recombinant chimeric viruses. Here, we report that the emergence of the rapid-high/SI phenotype for SIVMne is determined by changes in Gag and the Env transmembrane protein (Env TM) cytoplasmic tail region.

MATERIALS AND METHODS

Molecular cloning of an SIVMne variant from PBMCs. Peripheral blood mononuclear cells (PBMCs) were isolated from a pig-tailed macaque (*Macaca nemestrina*) infected with the pathogenic molecular clone SIVMneCL8 at 170 weeks postinoculation (1, 36, 41, 43). At this time, the macaque (M87004) had depressed CD4$^+$ T-cell counts and AIDS. The PBMCs were cocultured with the CD4$^+$ human T-B hybrid cell line, CEMx174, for 4 weeks (M87004 170 week [CEM]) (43, 45). The phenotype of the virus population in this coculture has

* Corresponding author. Mailing address: Department of Microbiology, Box 357242, University of Washington, Seattle, WA 98195-7242. Phone: (206) 543-3146. Fax: (206) 543-8297. E-mail: overbaug@u.washington.edu.

been previously described and is similar to that of viruses present in cocultures with naive macaque PBMCs (43). Furthermore, the Env SU genotype was maintained in the CEMx174 coculture, suggesting that no obvious selection for particular variants had occurred (45). To obtain a full-length infectious molecular clone variant of SIVMneCL8 from this coculture, we digested high-molecular-weight genomic DNA prepared from the cocultured cells with *Eco*RI, ligated it into the *Eco*RI site of the λ DASH II arms (Stratagene, La Jolla, Calif.), and packaged the vector with the Gigapack XL II system (Stratagene). Approximately 2×10^6 plaques were screened with ^{32}P-labeled *gag-pol* and *env* DNA probes derived from the plasmid clone of the parent, SIVMneCL8 (pMneCL8). Plaques that scored positive for both probes on the primary screen were isolated and were further purified and amplified. Only one phage clone contained a full-length provirus, which we designated SIVMne170. This provirus was excised from the λ DASH II vector with *Eco*RI and ligated into the *Eco*RI sites of pUC18 (pSIVMne170). A partial restriction map of the variant was generated (Fig. 1). The sequence of the *gag* and *env* genes was determined by manual sequencing with the Sequenase version 2.0 kit (United States Biochemical, Cleveland, Ohio).

Construction of chimeric viruses. To construct recombinant viruses between the parent virus SIVMneCL8 and variant SIVMne170, conserved restriction sites were utilized. The restriction site positions, referred to throughout the text, are derived from the sequence of SIVMneCL8 (GenBank accession no. M32741). To produce construct 8/170, a *Bst*BI (5343)-to-*Sph*I (located in the pUC18 polylinker) fragment that includes sequences of SIVMne170 from *vpx* through the cellular flanking sequences downstream of the 3′ long terminal repeat (LTR) was excised from pSIVMne170 and inserted into the *Bst*BI and *Sph*I sites of pMneCL8. For construction of the reciprocal chimeric virus 170/8, a *Bst*BI-*Sph*I fragment of pMneCL8 was ligated into the *Bst*BI and *Sph*I sites of pSIVMne170. For clone 8/170xr-su, the *Bst*BI (5343)-*Cla*I (7546) fragment in pMneCL8 that contains the *vpx-vpr-tat-rev-env* SU sequences was removed and replaced by the homologous sequences from SIVMne170. For clone 8/170env, the *Nsi*I (6392)-*Kpn*I (8847) fragment in pMneCL8 that contains *env*, except for the region encoding the Env leader sequence, was replaced with those sequences from SIVMne170. For recombinant virus 8/170su, the *Nsi*I (6392)-*Cla*I (7546) *env* SU from pMneCL8 was replaced with the homologous sequences from pSIVMne170 by previously described methods (44). To construct 8/170tm-ecto, the *Cla*I (7546)-*Nhe*I (8216) fragment that encodes the ectodomain and the membrane-spanning domain of Env TM was excised from pMneCL8 and replaced with the homologous sequences from pSIVMne170. For clone 8/170tm-tail, a *Nhe*I (8216)-*Kpn*I (8847) fragment that contains the 3′ region of the *env* TM gene was removed from pMneCL8 and replaced with the homologous region from pSIVMne170. To construct clone 8/170gag, the region of *gag* between *Dra*III (851) and *Nsi*I (1886) that includes the *gag* capsid (CA) and nucleocapsid (NC) sequences was excised from pMneCL8 and replaced with the homologous sequences from pSIVMne170. For clone 8/170pr, the 5′ region of *pol* that includes protease (PR) and the 5′ portion of reverse transcriptase was removed from pMneCL8 with *Nsi*I (1886) and *Hpa*I (3868) and replaced with the homologous sequence from pSIVMne170. The *vif* chimera 8/170vif was constructed by removing the *Bgl*II (4909)-to-*Bst*BI (5343) internal region of *vif* from pMneCL8 and replacing it with the homologous sequence from pSIVMne170. Chimera 8/170ca was constructed by removing a *Dra*III (851)-*Hin*dIII (1441) fragment from pMneCL8 that encodes from amino acid 108 in the Gag polyprotein matrix (MA) region to amino acid 304 in the CA region and replacing it with the homologous sequences from pSIVMne170. The clone 8/170nc was made by removing the *Hin*dIII (1441)-to-*Nsi*I (1886) *gag* sequence, which encodes the carboxyl-terminal portion of CA through the amino-terminal sequence of p6 (amino acids 305 to 452 of the Gag polyprotein), from pMneCL8 and replacing it with the homologous region from pSIVMne170. For clones 8/170env, 8/170su, 8/170tm-tail, 8/170gag, 8/170pr, 8/170vif, 8/170ca, and 8/170nc, multiple cloning steps were required to engineer the indicated changes. Partial sequencing and restriction mapping of the chimeric clones confirmed the presence of the SIVMne170 sequences in the background of SIVMneCL8.

Overlap extension mutagenesis. To convert a stop codon (codon 737 of SIVM neCL8 *env*) in the *env* TM intracytoplasmic tail region to a Gln codon, site-directed mutagenesis was performed according to the PCR overlap extension mutagenesis protocol of Ho et al. (23). Briefly, a subclone of SIVMneCL8 in Bluescript pKS$^+$ (Stratagene) that contains the 3′ end of the provirus from a *Hin*dIII site in *env* SU to a *Sal*I site in the cellular flanking sequences downstream of the LTR (plasmid p64-5) was used as a template for PCR amplification. For the first-round PCRs, DNA fragments surrounding the premature translational stop codon were generated with the PCR primer combinations of SIV-Env 34 (5′-TGGCAGAACTGTATCGATTGGATT-3′; nucleotide positions 7535 to 7559)/SIV-R-TMT/C-1 (5′-ATGGGTCT***G***CTGGAAATAAGA AGG-3′; nucleotide positions 8285 to 8262) and SIV-F-TMT/C-2 (5′-ATTTC CAG***C***AGACCCATATCCGAC-3′; nucleotide positions 8269 to 8892)/SIV-Env 32 (5′-TTCTTAAGGGAACTCGTGGCCTCA-3′; nucleotide positions 8854 to 8878). SIV-R-TMT/C-1 and SIV-F-TMT/C-2 are the overlapping primers that contain the specific mutation that changes the premature stop codon at amino acid position 737 to a Gln codon. The mutant bases (C and G; position 8277 of SIV-F-TMT/C-2 and SIV-R-TMT/C-1, respectively) are indicated in bold italicized letters. For the first round of amplification, an initial cycle of denaturation was performed at 94°C for 4 min, followed by 35 cycles of amplification. Each cycle consisted of DNA denaturation at 94°C for 1 min, annealing at 56°C for 1 min, and extension at 72°C for 2 min. The expected DNA products were mixed, diluted, and subjected to a second round of PCR with primers SIV-Env 32 and SIV-Env 34 for amplification. The DNA templates were denatured at 94°C for 4 min and then amplified for 35 cycles. Each cycle consisted of DNA denaturation at 94°C for 1 min, annealing at 45°C for 2 min, and extension at 72°C for 2 min.

The resulting product was digested with *Nhe*I and *Kpn*I and cloned into the *Nhe*I and *Kpn*I sites of p64-5. Five clones were screened for the presence of the T-to-C mutation in position 1 of codon 737 by DNA sequencing. A clone containing only the T-to-C mutation was digested with *Nhe*I and *Sal*I. These viral sequences were ligated into the complementary *Nhe*I and *Sal*I sites in the parent virus SIVMneCL8 to produce a provirus that expresses a full-length Env TM intracytoplasmic tail.

Virus stocks. Ten million CEMx174 cells were transfected with 10 μg of each plasmid proviral construct by the DEAE-dextran method and cultured for 10 days in RPMI complete medium (RPMI 1640 supplemented with 10% heat-inactivated [56°C for 30 min] fetal bovine serum, 2 mM L-glutamine, 100-U/ml penicillin, 100-μg/ml streptomycin, and 250-ng/ml amphotericin B). Conditioned viral supernatants were clarified by centrifugation at 1,500 rpm for 10 min in a Beckman GS-6R clinical centrifuge, filtered with 0.22-μM-pore-size filters (Millipore, Bedford, Mass.), and stored in 1-ml aliquots at −70°C. The tissue culture infectious dose (TCID) per milliliter of each virus supernatant stock was determined by the sMAGI assay (5). Briefly, sMAGI indicator cells were infected with 2 to 50 μl of viral supernatant and stained for β-galactosidase expression 3 days postinfection to detect infected cells as previously described (5).

Infection of human CD4$^+$ cell lines. The human CD4$^+$ T-cell lines Molt4 Clone 8, MT4, CEM, and Jurkat and a CD4$^+$ T-B-cell hybrid cell line, CEMx174, were maintained in RPMI complete medium. To examine viral tropism for these cell lines, triplicate cultures of 5×10^5 cells from each line were infected with 1,000 TCIDs of each virus derived from the molecular clones of SIVMne and propagated in 2 ml of RPMI complete medium. Every 3 days, 1 ml of medium was removed from each culture, the cell numbers were adjusted to 5×10^5 total cells, and fresh medium was added to 2 ml. If there were cytopathic effects in a culture that reduced the total cell number below 5×10^5 cells, then no cells were removed, but 1 ml of culture medium was removed and replaced with 1 ml of fresh medium. At 6, 12, and 18 days postinfection, 1 ml of supernatant from each culture was saved and stored at −70°C. Viral replication was assessed by examining the supernatants for cell-free SIV p27^{gag} by antigen enzyme-linked immunosorbent assay (ELISA) specific for the SIV p27^{gag} capsid protein (Immunotech, Westbrook, Maine). Cultures were scored positive for viral replication if the cell-free supernatants taken at 12 and 18 days postinfection were positive for SIV p27^{gag} (>50 pg/ml).

Replication and cytopathicity of SIVMne variants in CEMx174 cells. To compare the replication rates and cytopathicity of the different viruses in a CD4$^+$ cell line, duplicate cultures of 8×10^5 CEMx174 cells were infected with 200 TCIDs of each virus for 4 h in RPMI complete medium. Following the incubation, the cells were pelleted by centrifugation at 1,200 rpm in a Beckman GS-6R clinical centrifuge, washed twice with phosphate-buffered saline to remove residual free virions, and resuspended in 2 ml of fresh RPMI complete medium. Every 2 to 3 days, both the viable and total cell numbers were determined by trypan blue dye exclusion, and the total number of syncytia per culture was counted by visual inspection at a magnification of ×100 with an inverted phase-contrast microscope (Nikon). Only syncytia larger than 5 cell diameters were scored. Viral replication was monitored by assaying dilutions of the culture supernatants for cell-free SIV p27^{gag} by antigen ELISA. Only the p27^{gag} values that were obtained in the linear range of the assay were used for calculating the amount of p27^{gag}. The cell number in each culture was adjusted to 8×10^5, and fresh RPMI complete medium was added to a final volume of 2 ml. If the cell number was below 8×10^5, then no cells were removed, but one-half of the culture medium was replaced with fresh RPMI complete medium.

Isolation and infection of PBMCs and monocytes/macrophages. Macaque PBMCs were isolated from whole blood of SIV- and simian type D retrovirus-negative pig-tailed macaques (*M. nemestrina*) by Ficoll-Hypaque centrifugation as previously described (43). To examine viral replication in PBMCs, PBMCs were cultured with 10 μg of phytohemagglutinin (PHA) P (Difco Laboratories, Detroit, Mich.) per ml in RPMI complete medium supplemented with 20-U/ml human recombinant interleukin 2 (IL-2) (Boehringer Mannheim, Indianapolis, Ind.) for 3 days. The cells were pelleted by centrifugation at 1,200 rpm in a Beckman GS-6R clinical centrifuge and washed with RPMI complete medium to remove the PHA, and duplicate cultures of 2×10^6 cells were infected with 2,000 TCIDs of each virus in 1 ml of RPMI complete medium plus 20 U of IL-2 per ml. The following day, the cells were pelleted, washed with phosphate-buffered saline twice to remove residual cell-free virions, and resuspended in 3 ml of RPMI complete medium supplemented with 20 U of IL-2 per ml. Every 3 days, 2 ml of culture supernatant was removed and replaced with fresh RPMI complete medium plus IL-2 (20 U/ml). The supernatants were stored at −70°C and assayed for cell-free SIV p27^{gag} antigen by ELISA.

To analyze the cytopathicity of the viruses for CD4$^+$ T cells, 4×10^6 PBMCs were infected with each virus with a multiplicity of infection (MOI) ranging from 0.001 to 0.1. Over a 2-week period, the percentage of CD4$^+$ T cells in each of the cultures was monitored by fluorescence-activated cell sorting (FACS) analysis with a Becton Dickinson FACScan (San Jose, Calif.). For the analysis, 30,000

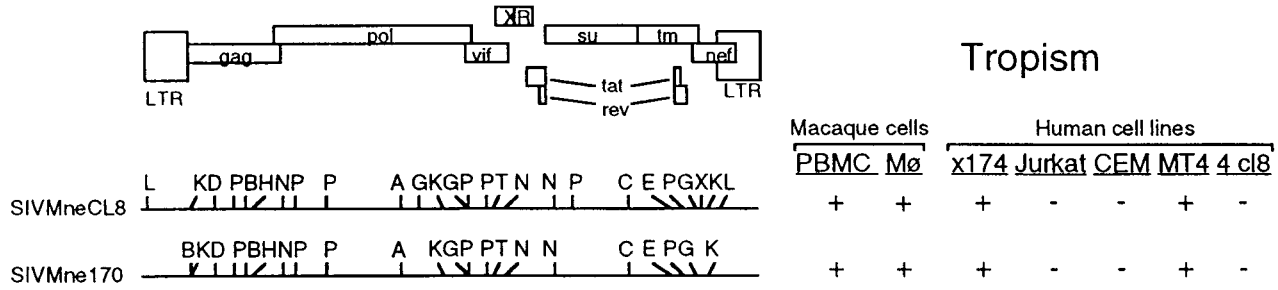

FIG. 1. Comparison of the structure and infectivity of SIVMneCL8 and the peripheral blood-derived variant SIVMne170. A schematic diagram of the SIV proviral genome is shown, and below it are restriction maps of SIVMneCL8 and variant SIVMne170. A, *Hpa*I; B, *Bam*HI; C, *Cla*I; D, *Dra*III; E, *Nhe*I; G, *Bgl*II; H, *Hin*dIII; K, *Kpn*I; L, *Bgl*I; N, *Nsi*I; P, *Pst*I; T, *Bst*BI; X, *Xho*I. To examine tropism, macaque PBMCs, macaque monocytes/macrophages (Mϕ), or the human CD4$^+$ cell lines CEMx174 (x174), Jurkat, CEM, MT4, and Molt4 Clone 8 (4 cl8) were infected at a low MOI (0.001). Replication was monitored as described in Materials and Methods by antigen ELISA for SIV p27^{gag}. A plus sign indicates an SIV p27^{gag}-positive culture, and a minus sign indicates an SIV p27^{gag}-negative culture.

cells were counted. Forward and side scatter light characteristics were used to exclude dead cells from the analysis. Anti-human CD4 and anti-human CD8 monoclonal antibodies (Becton Dickinson) that cross-react with macaque CD4 and CD8, respectively, were used for enumeration. An anti-macaque CD3 monoclonal antibody was obtained from Biosource International (Camarillo, Calif.).

Monocytes/macrophages were isolated from macaque PBMCs by adherence to plastic tissue culture flasks (Corning, Corning, N.Y.), cultured for 5 days in macrophage medium (RPMI 1640 supplemented with 10% heat-inactivated [56°C, 30 min] human type AB serum, 5% heat-inactivated fetal bovine serum, 10% GCT-conditioned medium [obtained from the AIDS Research Reagent and Reference Program], 2 mM glutamine, 100-U/ml penicillin, 100-mg/ml streptomycin, and 250-ng/ml amphotericin B), and infected as previously described (43). Duplicate cultures were infected with each virus with an MOI of 0.001. Viral replication was monitored by assaying supernatants taken at 3- to 4-day intervals postinfection for the presence of SIV p27^{gag} by ELISA.

Nucleotide sequence accession numbers. The complete nucleotide sequences of the *gag* and *env* genes of SIVMne170 were entered into GenBank under accession no. U95965 and U95966, respectively.

RESULTS

Characterization of a PBMC-derived variant of SIVMne CL8. To obtain an infectious molecular clone of a rapid-high/SI variant virus that evolved during the development of simian AIDS, we isolated a proviral clone from a coculture that expresses rapid-high/SI variants of SIVMneCL8. A partial restriction map of the late variant virus, designated SIVMne170, was generated and compared with the parent virus, SIV MneCL8 (Fig. 1). Overall, many of the restriction sites were conserved between SIVMne170 and SIVMneCL8. However, the viruses could be distinguished from each other by restriction site polymorphisms scattered throughout the genome. For example, relative to SIVMneCL8, the variant SIVMne170 contained an additional *Bam*HI site in the untranslated sequence between U5 and the *gag* initiation codon but had lost *Bgl*II, *Pst*I, *Xho*I, and *Bgl*I sites in *pol*, *env*, *nef*, and LTRs, respectively. Finally, a spreading infection was observed when CEMx174 cells were transfected with the SIVMne170 proviral clone, demonstrating that SIVMne170 was replication competent (data not shown).

To compare the host cell tropism of SIVMne170 and SIVM neCL8, various human CD4$^+$ T-cell lines, macaque PBMCs, and macaque monocyte/macrophage cultures were infected with an equal infectious dose of each virus (MOI, 0.001). The viruses displayed similar host cell ranges for the macaque and human cells. Both viruses were capable of replicating in cultures of pig-tailed macaque monocytes/macrophages and PHA-stimulated pig-tailed macaque PBMCs, the human hybrid cell line CEMx174, and the human T-cell leukemia virus type 1 (HTLV-1)-transformed cell line MT4. Neither virus replicated in the Jurkat, CEM, or Molt4 Clone 8 cell line.

We previously demonstrated that the CEMx174 cell line could be used to identify rapid-high/SI viruses (43). To determine whether SIVMne170 had an increased ability to replicate and to cause syncytia and cytopathic effects compared to the slow-low/NSI parent virus, SIVMneCL8, we infected CEMx174 cells at an equal MOI with each virus and monitored their phenotype (Fig. 2). The peak level of SIVMne170 p27^{gag} occurred 2 to 3 days before that of SIVMneCL8 but dropped off to a low level by 18 days postinfection (Fig. 2A). However, the p27^{gag} level of SIVMneCL8 rose to a level twofold higher than that of SIVMne170. The differences in steady-state levels may, in part, reflect the cytopathic effects of SIVMne170. For example, when the p27^{gag} values were adjusted by the number of viable cells, SIVMne170 produced a greater amount of p27^{gag} per cell (five- to sevenfold) than SIVMneCL8 (data not shown).

In the SIVMne170-infected CEMx174 cultures, a decrease in the viable cell number began concomitant with the peak in the level of p27^{gag} expression. This decrease was reflected both in the extrapolated viable cell number (Fig. 2B), which decreased approximately 1,000-fold compared to the uninfected cultures, and in the percentage of cells that were viable (Fig. 2C), which decreased to less than 5%. The cytopathic effects of the parent virus, SIVMneCL8, also coincided with its peak p27^{gag} antigen level. However, its cytopathic effects were modest; it decreased the viable cell number by fivefold (Fig. 2B). Furthermore, the cell viability remained greater than 45% throughout the course of the infection (Fig. 2C). Syncytia were also observed at the peak level of p27^{gag} antigen production in the SIVMne170 cultures, but few were found in the SIVM neCL8-infected cultures (Fig. 2D). Similar results were obtained in 10 independent experiments. Together, these data demonstrate that SIVMne170 represents a rapid-high/SI variant that evolved from the minimally cytopathic, NSI, parent virus SIVMneCL8. SIVMne170 is therefore an appropriate virus for identifying the genetic changes that confer an increase in viral replication and cytopathicity on variant viruses that are selected during progression to AIDS.

5′ and 3′ determinants confer a cytopathic phenotype upon SIVMne170. To identify the determinants in SIVMne170 that conferred its rapid-high/SI phenotype, we constructed recombinant chimeric viruses between SIVMne170 and the parent virus, SIVMneCL8, by using conserved restriction sites in the proviral genomes (Fig. 3). Initially, the simplest reciprocal chimeric viruses (8/170 and 170/8), which exchange the coding regions for *gag-pol*-5′-*vif* and 3′-*vif-vpx-vpr-tat-rev-env-nef*-LTR regions, were constructed and analyzed. Recombinant 8/170, which contained the 5′ half of SIVMneCL8 and the 3′ half of SIVMne170, replicated with similar kinetics as SIVMneCL8.

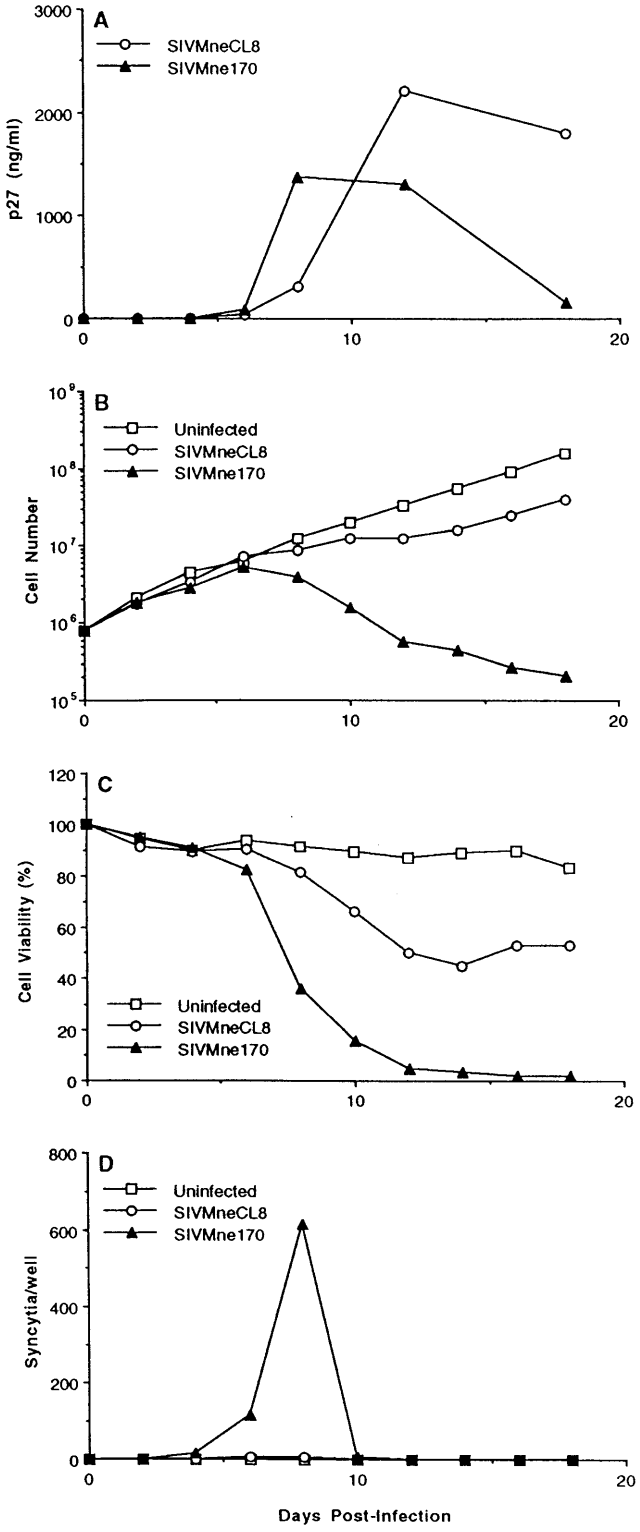

FIG. 2. Comparison of the replication kinetics, cytopathicity, and SI ability of SIVMneCL8 and SIVMne170 in CEMx174 cells. Eight hundred thousand CEMx174 cells were infected with 200 TCIDs of either SIVMneCL8 or SIVMne170. At 2-day intervals postinfection, SIV $p27^{gag}$ production was monitored by antigen ELISA (A), the extrapolated viable cell number (B) and cell viability (C) were determined by trypan blue dye exclusion, and the total number of syncytia (D) were counted in each culture as described in Materials and Methods. Each value shown is the average of duplicate cultures.

However, like SIVMne170, 8/170 was SI and more cytopathic than SIVMneCL8, reducing the cell viability to 19% compared to 50% for SIVMneCL8; nevertheless, 8/170 was slightly less cytopathic than SIVMne170, which reduced the cell viability to 10%. The reciprocal chimeric virus, 170/8, replicated with kinetics similar to those of SIVMne170. Interestingly, even though 170/8 was NSI, it remained as cytopathic for CEMx174 cells as the parent virus SIVMne170, reducing the cell viability to approximately 9%. Together, these data demonstrated that cytopathic determinants are located in both the 5′ and 3′ halves of SIVMne170 and that the cytopathic effects of the virus can occur independent of either an enhanced replication rate or SI capacity.

To localize the 3′ determinants that contributed to the cytopathic SI phenotype of SIVMne170, we constructed chimeric viruses that included smaller regions of the 3′ half of the SIVMne170 proviral genome in the background of the parent virus SIVMneCL8 (Fig. 3). Like chimera 8/170, all of the chimeric viruses with a 3′ region derived from SIVMne170 replicated with similar efficiency as SIVMneCL8, except for 8/170su, which contained only the *env* SU region from SIVMne170. Recombinant 8/170su replicated with delayed kinetics compared to SIVMneCL8; its $p27^{gag}$ antigen level peaked 3 to 4 days later than SIVMneCL8 and 5 to 6 days later than SIVMne170, similar to other chimeric viruses that contained the *env* SU region of other late variant viruses (44). When these chimeric viruses were examined for their SI ability, only the recombinants that expressed either the SU or the TM intracytoplasmic tail region of the SIVMne170 *env* were capable of inducing syncytia (Fig. 3 and 4). These viruses included 8/170xr-su, 8/170env, 8/170su, and 8/170tm-tail. By contrast, a chimeric virus, 8/170tm-ecto, expressing only the ectodomain of the *env* TM from SIVMne170 did not confer the SI phenotype. Interestingly, when the chimeric viruses harboring 3′ determinants from SIVMne170 were examined for the ability to cause cytopathic effects, only the chimeric viruses that expressed the intracytoplasmic tail-encoding region of *env* TM from SIVMne170 were capable of significantly enhancing the cytopathicity of SIVMneCL8. These viruses included 8/170env and 8/170tm-tail, which decreased the cell viability to 30 and 18%, respectively. Together, these data demonstrate that within the 3′ end of the viral genome both *env* SU and TM contribute to the SI phenotype of SIVMne170 but that only the cytoplasmic tail-encoding region of *env* TM harbors a cytopathic determinant.

To identify the 5′ determinant(s) in SIVMne170 that conferred its rapid replication kinetics and contributed to its cytopathicity, we constructed and analyzed chimeric viruses that contained regions of *gag*, *pol*, or *vif* from SIVMne170 but were isogenic with respect to SIVMneCL8 (Fig. 3). The chimeric viruses that contained the *gag* CA and NC (8/170gag), PR and 5′ region of reverse transcriptase from *pol* (8/170pr), or *vif* (8/170vif) regions from SIVMne170 replicated with faster kinetics than SIVMneCL8 in CEMx174 cells, suggesting that mutations in each of these determinants independently contributed to the rapid replication kinetics of SIVMne170. However, of these three chimeric viruses only the recombinant containing the *gag* CA and NC regions from SIVMne170 (8/170gag) was significantly more cytopathic than SIVMneCL8, reducing the cell viability to 27% compared to 50% by SIVMneCL8.

To further define the 5′ cytopathic determinant, the *gag* determinant was subdivided. The resulting recombinant viruses contained sequences primarily from either the *gag* CA (virus 8/170ca) or *gag* NC (virus 8/170nc) of SIVMne170 and were isogenic with respect to SIVMneCL8. Both of these chi-

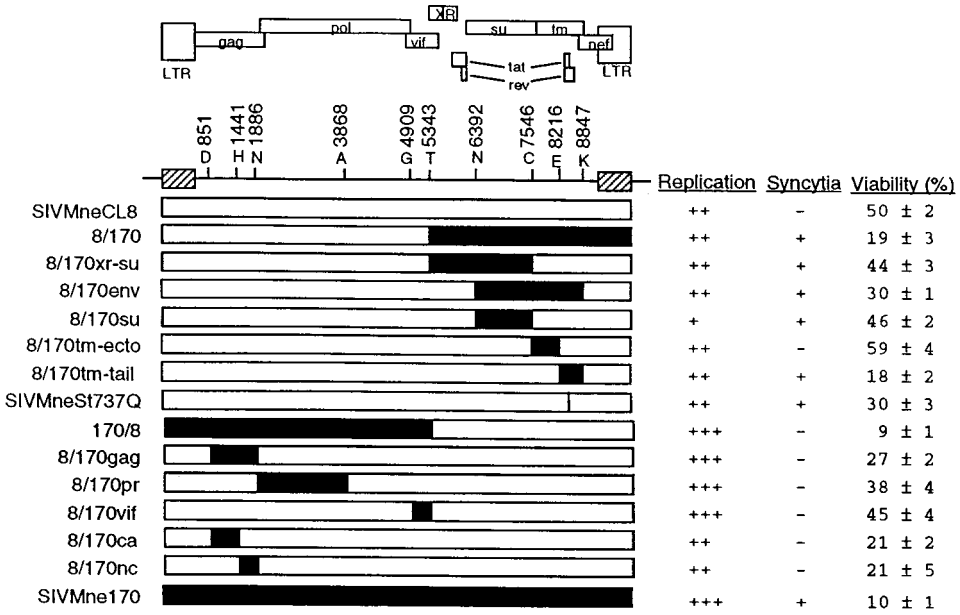

FIG. 3. Replication, cytopathicity, and SI capacity of chimeric viruses in CEMx174 cells. Recombinant chimeric proviruses were constructed by using restriction sites conserved between SIVMneCL8 and SIVMne170. Each restriction site and its position are indicated on a linear provirus depicted below the schematic diagram of the SIV reading frames. Chimeric viruses are indicated in black and white boxes. Black boxes indicate regions of the SIVMne170 genome cloned into the background of the parent virus SIVMneCL8 (open boxes). Replication, cytopathicity, and syncytium induction were monitored as described in the legend to Fig. 2. For viral replication, the replication kinetics of each virus relative to that of the parent SIVMneCL8 (represented by two plus signs) is shown. Thus, a single plus sign indicates a peak SIV $p27^{gag}$ antigen level 3 to 4 days later than that of SIVMneCL8 (++), two plus signs indicate an equal rate of replication, and three plus signs indicate that the peak SIV $p27^{gag}$ antigen level occurred 2 to 3 days earlier than that found for SIVMneCL8. For syncytium induction, a minus sign indicates that the average number of syncytia was less than 25 per culture and a plus sign indicates that the average number of syncytia was greater than 400 per culture. The values shown under the viability (percent) column represent the lowest percentages of viable cells plus or minus the standard errors of the means rounded to the nearest whole number. The numbers in each column are the average values calculated from a minimum of four independent infections. All infections were monitored for 15 to 18 days.

meric viruses replicated with kinetics similar to SIVMneCL8 but were significantly more cytopathic than SIVMneCL8, reducing the cell viability to approximately 21%. The decrease in cell viability induced by either 8/170ca or 8/170nc was not as pronounced as the reduction in cell viability to 10% caused by SIVMne170 or the chimera 170/8 but was similar to 8/170gag. Finally, none of the recombinant viruses harboring 5′ determinants from SIVMne170 caused syncytia, suggesting that these determinants did not influence the SI property. Together, these data demonstrate that mutations in *gag* CA and NC, *pol*, and *vif* independently influence the replication kinetics of SIVMne170 in CEMx174 cells but that the primary 5′ cytopathic determinants map to the *gag* CA and NC regions.

Sequence analysis of the *gag* and *env* genes from SIVMne 170. To identify the specific mutations in *gag* and *env* that may be important for the rapid-high/SI phenotype of SIVMne170, we compared the predicted amino acid sequences of *gag* and *env* from SIVMne170 with those sequences of the parent virus, SIVMneCL8. Eight amino acid differences in the Gag sequence (positions 61, 116, 140, 259, 282, 391, 408, and 504) distinguished the SIVMne170 Gag from the SIVMneCL8 Gag (Fig. 5). Four of the mutations are nonconservative (E116A, S282N, T408A, and E504G). Only two of the mutations in SIVMne170, N-282 in CA and A-408 in the linker region between the two zinc-finger, Cys-His boxes of NC, converted amino acids to ones that are highly conserved among the SIVs (37). Both of these mutations were present in the *gag* determinant from SIVMne170 that was inserted into the background of the parent virus SIVMneCL8 to produce the chimeric virus 8/170gag. Also, N-282 was encoded in the *gag* CA fragment of SIVMne170 present in 8/170ca, and A-408 was encoded in the *gag* NC fragment of SIVMne170 present in 8/170nc. Thus, these mutations may have roles in increasing the replication rate and cytopathicity of SIVMne170.

Within envelope extracellular protein, amino acid differences between SIVMneCL8 and SIVMne170 were most extensive in variable regions V1 and V4 (Fig. 6). These mutations are characteristic of those that we have previously reported for SI variant virus populations of SIVMne (41, 43–45). Specifically, the mutations in V1 may potentially alter O-linked and N-linked glycosylation, particularly the P132S and N149S mutations (4, 40). Furthermore, the N416D and T418N mutations are predicted to shift an N-linked glycosylation site in V4.

Within the envelope transmembrane protein, SIVMne170 contains several mutations that distinguish it from SIVM neCL8 (Fig. 6). In the ectodomain, there are three mutations (positions 630, 634, and 645), one of which (N630S) shifts a potential N-linked glycosylation site. However, this change did not appear to have any bearing on either the SI property or the cytopathicity of SIVMne170 because chimeric virus 8/170tm-ecto (Fig. 3) was NSI and no more cytopathic than SIVM neCL8. Additionally, there are no mutations in the fusion peptide (2) of the SIVMne170 Env TM that could account for the change in viral phenotype from that of SIVMneCL8.

The most notable difference between the Env TM of SIVM neCL8 and that of variant SIVMne170 is the reversion of a premature stop codon to a Gln at position 737 within the intracytoplasmic tail. The reversion results from a thymine-to-cytosine change at position 1 of codon 737 of *env*. The mutation is predicted to allow expression of the carboxyl-terminal portion of the Env TM intracytoplasmic tail that includes the highly conserved palmitoylation site at 790 (54) and the lentiviral lytic peptide region (33, 34, 54). However, it does not

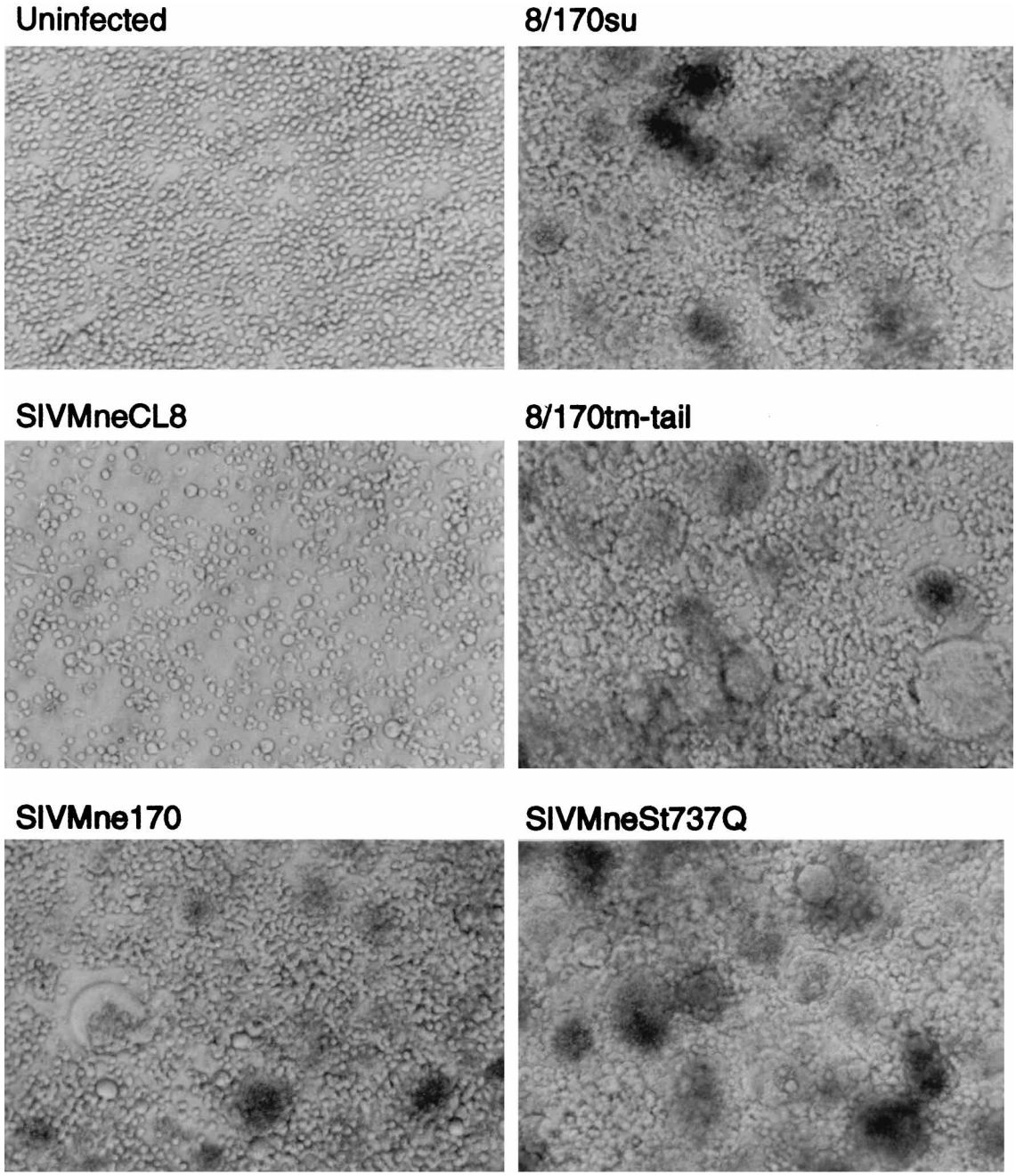

FIG. 4. SI capacity of chimeric viruses. CEMx174 cells (8×10^5) were infected with 200 TCIDs of each of the viruses shown. At 8 days postinfection, the cultures were examined for syncytia, and photographs were taken with an inverted phase-contrast microscope (magnification, ×100).

affect alternative overlapping reading frames such as those for *tat*, *rev*, and *nef* or the Rev response regulatory element.

To determine whether the reversion of the premature stop codon in the *env* TM to a Gln codon was common to variants of SIVMneCL8, we sequenced the *env* TM intracellular domain of PCR-amplified clones from sequential PBMC samples of macaque M87004. A cytosine in position 1 of codon 737 was observed in each variant examined from two time points (data not shown). The earliest clones were obtained from a PBMC sample taken at 35 weeks postinoculation, 8 weeks prior to $CD4^+$ T-cell decline, suggesting that the reversion occurred early as shown by others (22, 27).

Env TM intracytoplasmic tail is a determinant of cytopathicity and syncytium induction. To determine whether a reversion of the premature stop codon in the SIVMneCL8 *env* TM would confer an SI phenotype and enhance cytopathicity, we changed the *env* stop codon 737 to one encoding Gln and examined the phenotype of the mutant virus in CEMx174 cells. Expression of a full-length Env TM by the mutant, designated SIVMneSt737Q, was confirmed by Western blot analysis (data not shown). Mutant SIVMneSt737Q replicated with kinetics similar to the parent virus, SIVMneCL8. However, SIVMne St737Q was SI and more cytopathic than SIVMneCL8 (Fig. 3 and 4), reducing the cell viability to 30%. These data demon-

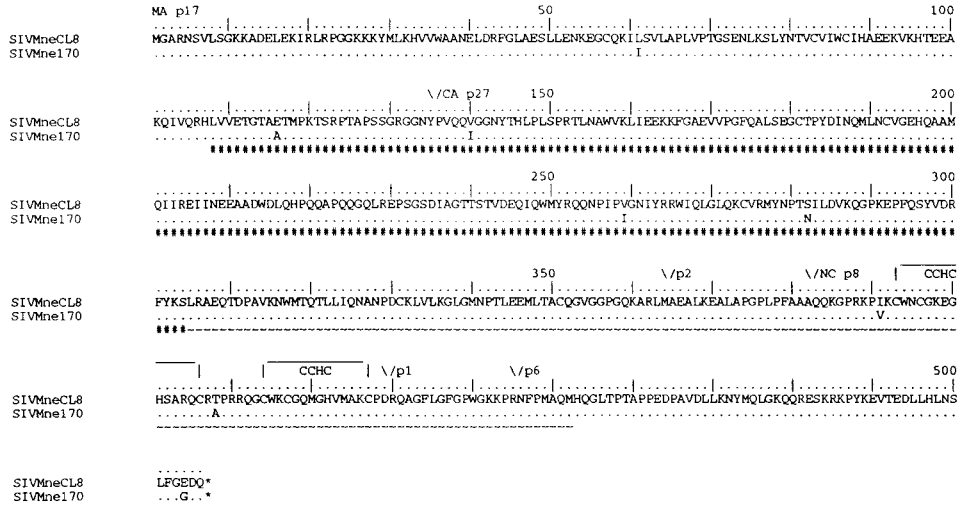

FIG. 5. Comparison of the predicted amino acid sequences of the Gag polyprotein from SIVMneCL8 and SIVMne170. The Gag sequence of the parent virus SIVMneCL8 serves as the reference sequence and is shown in single-letter code. The amino acid number is shown above the sequence. Amino acids in the variant virus SIVMne170 Gag that are identical to those in SIVMneCL8 are represented by dots. Specific amino acid differences are shown. Cleavage sites for the major Gag protein products are indicated above the sequences, and the Cys-His boxes in the nucleocapsid protein are shown (CCHC). An asterisk indicates the translational stop site. The symbols located under the predicted amino acid sequences denote the regions encoded by SIVMne170 that were introduced into chimeric viruses 8/170ca (#), 8/170nc (~), and 8/170gag (# and ~). MA, matrix; CA, capsid; NC, nucleocapsid.

strate that the intracytoplasmic tail of Env TM can be both a cytopathic and an SI determinant of SIV.

Replication rates and cytopathicity of SIVMneCL8 and SIVMne170 in PBMCs. To examine SIVMne170 and SIVM neCL8 replication in a more physiologically relevant cell population, we infected pig-tailed macaque PBMCs. Although SIVMne170 consistently replicated with faster kinetics than SIVMneCL8 in CEMx174 cells, in macaque PBMCs the differences in replication were variable and donor dependent (Fig. 7). For example, in macaque PBMCs from one animal, we found that the peak $p27^{gag}$ level from the SIVMne170-infected cultures was 100-fold higher than the level achieved in the SIVMneCL8-infected cultures, suggesting that SIVMne170 replicated to a higher level (Fig. 7A). However, in PBMCs from a second macaque donor, the $p27^{gag}$ antigen level for SIVMneCL8 was threefold higher than that of SIVMne170 (Fig. 7B). The different results in Fig. 7A and B were primarily due to SIVMneCL8's ability to replicate in the donors' PBMCs, because SIVMne170 replicated to a high level in the PBMCs from both macaque donors. Variable results similar to these were also observed when the replication kinetics of SIVMneCL8 and SIVMne170 from three other macaque PBMC infection experiments were compared with each other (data not shown).

Although SIVMne170 did not appear to consistently replicate to a higher level than SIVMneCL8 in macaque PBMCs derived from different donors, it was nevertheless more cytopathic for the $CD4^+$ T-cell population in all macaque PBMC cultures examined. When macaque PBMCs were infected with each virus at a low MOI (0.001), SIVMne170 reduced the $CD4^+$ T-cell population by 20% after 11 days of infection and by 33% by 14 days postinfection (Fig. 8A). In contrast, SIVM neCL8 did not reduce the percentage of $CD4^+$ T cells after 11 days of infection but caused a 12% reduction by 14 days postinfection. Similarly, when macaque PBMCs were infected at a 10-fold higher MOI with each virus, SIVMne170 remained more cytopathic for the $CD4^+$ T-cell population than SIVM neCL8 (Fig. 8B). SIVMne170 reduced the $CD4^+$ T-cell population by 45 and 53% after 8 and 15 days of infection, respectively, while SIVMneCL8 caused reductions of 26% after 8 days and 37% by 15 days postinfection. In additional infections of macaque PBMCs derived from different donors, SIVM ne170 was consistently more cytopathic for the $CD4^+$ T-cell population than SIVMneCL8 (data not shown). Furthermore, syncytia were not observed in any cultures of PBMCs infected with either SIVMne170 or SIVMneCL8 (data not shown). These data suggest that SIVMne170 is more cytopathic for primary macaque PBMCs than the parent virus, SIVMneCL8.

To determine whether the *gag* region of SIVMne170 was a cytopathic determinant for macaque primary $CD4^+$ T cells, we infected PHA-stimulated macaque PBMCs with the recombinant virus 8/170gag and examined its ability to kill $CD4^+$ T cells by FACS analysis (Fig. 8B). Recombinant 8/170gag reduced the $CD4^+$ T-cell population by 72% after 8 days and 78% by 15 days postinfection. This level of cell killing was more extensive than that of either SIVMneCL8, which reduced the $CD4^+$ T-cell population by 26 and 37% after 8 and 15 days of infection, respectively, or SIVMne170, which reduced the $CD4^+$ T-cell population by 45% after 8 days and 53% by 15 days postinfection. Similar observations were made in two additional independent experiments with PBMCs derived from two other macaque donors (data not shown). Neither *gag* chimera 8/170ca nor 8/170nc caused as high a level of $CD4^+$ T-cell killing as 8/170gag, although chimera 8/170nc was as cytopathic as SIVMne170 (data not shown). These data demonstrate that mutations in Gag influence the cytopathicity of SIVMne for primary macaque $CD4^+$ T cells.

We also determined whether mutant SIVMneSt737Q, which contained only a point mutation that changed the premature stop codon in the *env* TM intracytoplasmic tail of SIVMneCL8 to a full-length open reading frame, was more cytopathic for primary macaque $CD4^+$ T cells than the parent SIVMneCL8 (Fig. 8C). In contrast to SIVMneCL8, which reduced the $CD4^+$ T-cell population by 16% after 7 days and 50% by 13 days postinfection, mutant SIVMneSt737Q caused a 70% loss of $CD4^+$ T cells by 7 days postinfection. This value increased to 92% by 13 days postinfection. Similar observations were made in four other independent experiments with PBMCs

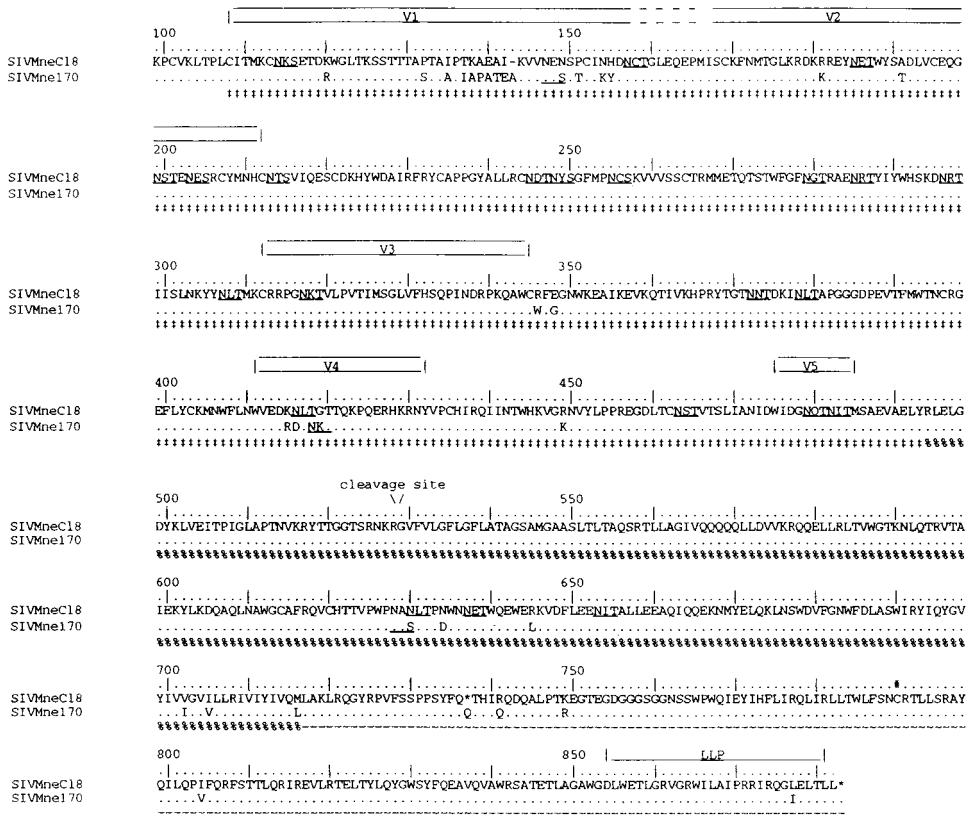

FIG. 6. Comparison of the predicted amino acid sequences of the envelope protein from SIVMneCL8 and SIVMne170. The predicted amino acid sequences from variable region 1 (V1) in envelope SU through the end of envelope TM are shown for SIVMneCL8. The amino acid number is shown above the sequence. Variable regions V1 through V5 are indicated by boxes above the sequences. The SU-TM cleavage site and lentiviral lytic peptide (LLP) regions are also indicated. Amino acids in SIVMne170 that are identical to those in SIVMneCL8 are represented by dots. Specific amino acid differences are shown. A dash indicates the absence of an amino acid, and an asterisk indicates a translational stop site. Potential N-linked glycosylation sites are underlined. The number sign indicates the conserved palmitoylation site. The symbols under the predicted amino acid sequences indicate the regions encoded by SIVMne170 that were introduced into chimeric viruses 8/170su (‡), 8/170tm-ecto (%), 8/170tm-tail (~), and 8/170env (‡, %, and ~).

from two different macaque donors (data not shown). Thus, these data demonstrate that the intracytoplasmic tail of Env TM is a determinant of cytopathicity for SIV. Finally, as we had previously found in CEMx174 cells, the chimeric virus expressing the Env SU from SIVMne170 in the background of SIVMneCL8 (8/170su) was minimally cytopathic for primary macaque $CD4^+$ T cells (data not shown).

DISCUSSION

SIVMne, like HIV-1, evolves from a slow-low/NSI virus, represented by SIVMneCL8, to a rapid-high/SI variant population as infected macaques progress to AIDS (43). Our previous studies showed that mutations selected in Env SU of SIVMneCL8 during the course of infection contribute to the shift from an NSI to an SI phenotype but do not enhance replication or cytopathicity (44). Therefore, in order to identify the determinants that affect the replicative and cytopathic properties of late variant viruses, we molecularly cloned a rapid-high/SI variant of SIVMneCL8 (designated SIVMne170) from a pig-tailed macaque with AIDS and used the variant to construct interviral recombinants with SIVMneCL8. Our analysis of the chimeric viruses demonstrated that several determinants in *gag* and *env* contributed to the rapid-high/SI phenotype of SIVMne170.

Our characterization of variant SIVMne170 showed that it was genetically and phenotypically different from the parent virus, SIVMneCL8. SIVMne170 displayed rapid replication kinetics and greater cytopathicity and SI ability compared to SIVMneCL8 in CEMx174 cells. SIVMne170 also demonstrated greater cytopathicity for the $CD4^+$ T-cell population in macaque PBMCs than SIVMneCL8, even though it did not consistently replicate to higher levels than SIVMneCL8 in these cells. A similar observation has been made for HIV-1 variants, although Connor et al. demonstrated that NSI HIV-1 variants replicate with slower kinetics and are less cytopathic than SI variants (11). For example, Yu et al. demonstrated that several HIV-1 M-tropic NSI viruses can replicate as well as, or faster than, T-cell-tropic SI viruses in PBMCs, but the extent of primary $CD4^+$ T-cell killing by M-tropic NSI viruses was less than that of T-tropic SI viruses (56). Thus, for both SIV and HIV-1, the ability to kill primary $CD4^+$ T cells may not correlate with the rate of virus replication, suggesting that other viral characteristics may contribute to cytopathicity. Furthermore, while SIVMne170 and SIVMneCL8 differ in their replication kinetics, cytopathicity, and SI properties, they displayed similar tropisms for primary macaque PBMCs and monocyte-derived macrophages and human $CD4^+$ cell lines. This phenotype is also similar to NSI and SI HIV-1 primary isolates and clones, which are dually tropic for monocyte-derived macrophages and PBMCs (9, 11, 17, 53). However, while there are some similarities in the phenotypes of HIV-1 and SIVMne variants, there is a difference in the methods used to

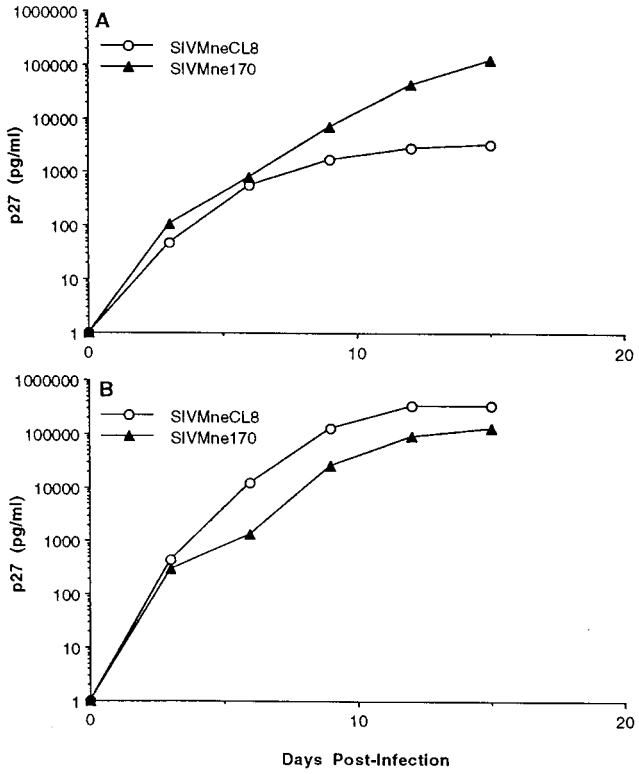

FIG. 7. Replication of SIVMneCL8 and SIVMne170 in macaque PBMCs. Duplicate cultures of 2×10^6 PHA-stimulated macaque PBMCs were infected with 2,000 TCIDs of each virus. Virus production was monitored at 3-day intervals by SIV $p27^{gag}$ antigen ELISA. Each value represents the average SIV $p27^{gag}$ value obtained from duplicate cultures. Different macaque PBMC donors were used for the infections shown in panels A and B.

examine the viral phenotypes. For SIVMne, we typically evaluate the SI phenotype in CEMx174 cells whereas the HTLV-1-transformed cell line, MT2, has been used for HIV-1 (11, 25, 28). We have shown here and previously that HTLV-1-transformed T-cell lines such as MT4 and C8166 (45) are infectable by SIVMne variants. Although the variants isolated at late stages of infection are both cytopathic and SI for C8166 cells, CEMx174 cells are a more sensitive indicator cell line for the cytopathic and SI effects of SIVMne (43). Together, these data further demonstrate that the virological changes that occur in SIVMne during the course of an infection are generally similar to those that occur in HIV-1.

The minimal determinants of SIVMne170 that were responsible for its SI phenotype mapped to the *env* gene. The SIVMne170 Env SU conferred an SI phenotype but did not contribute to the cytopathicity of SIVMne170 in either CEMx174 cells or macaque PBMCs. These data contrast with studies of HIV-1, demonstrating that mutations in Env SU, which confer an SI phenotype, are sufficient to increase cytopathicity (7, 12, 30, 32). However, the data are consistent with previous observations from our laboratory which showed that other chimeric SIVMne viruses, differing in their Env SU sequences but otherwise isogenic with respect to SIVMneCL8, are minimally cytopathic regardless of their NSI/SI phenotype (44). Thus, an SI Env SU does not appear to confer upon SIV greater cytopathicity than an NSI Env SU, and syncytium induction per se is not the primary cause of cell killing. Instead, a second SI determinant, which mapped to the intracellular domain of the SIVMne170 *env* TM gene, enhanced cytopathicity.

The ability of the Env TM intracellular domain to increase the cytopathicity of SIVMneCL8 contrasts with a previous study which suggests that a truncation of the cytoplasmic tail of Env TM does not affect the cytopathicity of SIVmac239 (27). The difference in results may be due to the cell lines used to examine the viral phenotype or a masking of the cytopathic effects of the Env TM intracytoplasmic tail by another cytopathic determinant in SIVmac239. A minimally cytopathic virus such as SIVMneCL8 may provide a better context for detecting the cytopathic effects contributed by the Env TM cytoplasmic tail. Interestingly, the carboxyl-terminal regions of both the SIV and HIV-1 Env TM intracytoplasmic tails are predicted to form amphipathic helices, and synthetic peptides of this region form pores in membranes and are cytotoxic for cells (8, 33, 34), suggesting that the intracellular domain of Env TM is a cytopathic determinant. Additional studies have shown that the cytoplasmic tail of the HIV-1 envelope protein binds calmodulin, raising the possibility that TM expression may disrupt signal transduction and cellular functions (35, 49, 50). Our data demonstrate that, in the context of a full-length replicating SIV, the Env TM intracytoplasmic tail may contribute to cell killing in macaque PBMCs and human cell lines. This is consistent with two studies of HIV-1 which also dem-

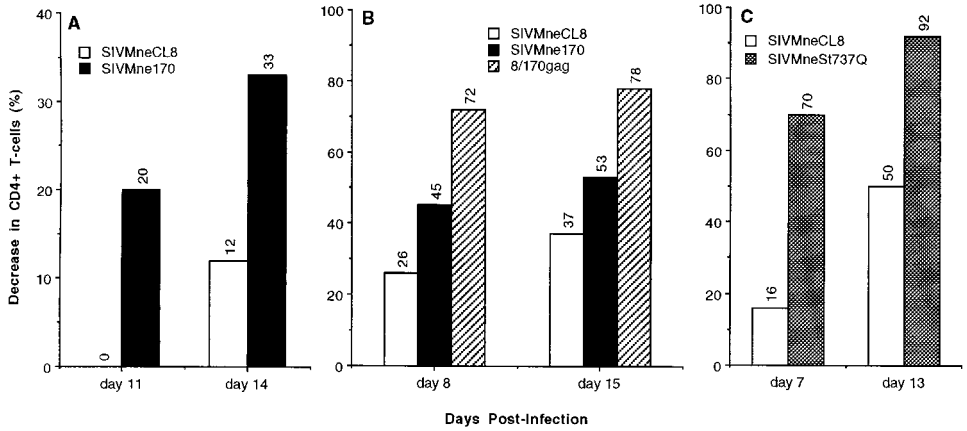

FIG. 8. Cytopathicity of SIVMne for primary macaque $CD4^+$ T cells. (A) PHA-stimulated macaque PBMCs were infected with each virus at an MOI of 0.001 (A) or 0.01 (B and C). At the indicated days postinfection, the decrease in $CD4^+$ T cells relative to the uninfected culture was determined by FACS analysis as described in Materials and Methods. The data shown in panels A, B, and C are from separate experiments with different macaque PBMC donors.

onstrated that mutations in the carboxyl-terminal region of Env TM affect cytopathicity (18, 29). However, using a heterologous Env expression system, another study of the HIV-1 Env TM suggests that the intracytoplasmic tail is not a cytopathic determinant (3). The difference in results may be explained by the methods or cell type used to express and examine the cytopathic effects of Env. Whether variation in this region of TM affects the cytopathicity and pathogenicity of SIV will be important to determine.

The function of the Env TM intracellular domain in viral replication is unclear. Studies from several groups have suggested that a truncation in the Env TM intracytoplasmic tail increases the rate of replication or expands tropism in human T-cell lines because it enhances the density of envelope proteins on virions compared to isogenic viruses with the full-length cytoplasmic tail (24, 58). Truncation of the Env TM intracytoplasmic domain has also been demonstrated to alter the conformation of the extracellular domain of Env TM, thereby possibly affecting envelope fusogenicity (48). Furthermore, syncytium induction has been shown to be greater for viruses with a truncation of the Env TM cytoplasmic tail (42, 58). Our data show that the presence of a full-length intracytoplasmic tail enhances Env fusogenicity as measured by syncytium induction. Thus, the selection for a full-length cytoplasmic tail in vivo may, in part, be driven by the requirement for an Env protein with greater fusogenicity. Additionally, the intracytoplasmic tail of Env TM may influence replication through other mechanisms. A study by Zhang et al. suggests that the cytoplasmic tail of HIV-1 increases viral infectivity by enhancing endogenous reverse transcription in virions (57). Whether this is true for SIV will be important to determine. Together, these data suggest that the Env TM intracytoplasmic tail plays an important role in viral replication by affecting fusogenicity, and perhaps infectivity. This is consistent with data presented here and those from earlier studies that demonstrate a strong selection in vivo for viruses encoding the intracytoplasmic domain of SIV Env TM (22, 27, 47). It should be noted, though, that Hirsch et al. (21) have recently showed that the predominant SIV variants cloned from brain tissue, but not peripheral blood, of a macaque infected with SIVsmE543-3 contain truncated Env TM intracytoplasmic tails. This demonstrates that de novo selection occurs in vivo for viruses with truncated Env TM intracytoplasmic tails and suggests a possible functional role for variants lacking a full-length Env TM.

The mutations in the Gag CA and NC of SIVMne170 conferred its faster replication kinetics and also contributed to its greater cytopathicity compared to the parent SIVMneCL8. Interestingly, the Gag determinants from SIVMne170 enhance the cytopathicity of SIVMneCL8 in the absence of syncytium formation. Thus, mutations in Gag may, in part, account for the high level of cytopathicity observed for some NSI viruses (26, 56). Both CA and NC play important roles in virus assembly and maturation (13, 14, 20, 39). In addition, NC facilitates reverse transcription and is a viral RNA-binding protein (13, 19, 55). Thus, it is possible that mutations in these regions could alter the replication kinetics of SIVMne by affecting both maturation and infectivity. How CA and NC affect the cytopathicity of the virus is unclear and will require further investigation. It is, however, unlikely that the *gag* determinant contributes to the cytopathicity of SIVMne170 simply by increasing virus production because the chimeric viruses harboring *pol* and *vif* determinants from SIVMne170 (8/170pr and 8/170vif) also replicated with faster kinetics than SIVMneCL8, but they were not more cytopathic.

In conclusion, we have demonstrated that the evolution of several determinants in SIVMneCL8 contributes to the emergence of the rapid-high/SI phenotype that is associated with rapid $CD4^+$ T-cell decline and AIDS. The identification of these mutations may now allow us to assess their independent contributions to pathogenicity in vivo. Thus, an important aspect of our approach is the examination of whether specific in vitro phenotypes such as rapid replication, increased cytopathicity, and SI ability are predictive of rapid disease progression. In this regard, it is interesting that the determinants of pathogenicity for the SIVmac and SIVsm strains have been shown to be complex (31, 38). However, those studies did not correlate specific changes in the in vitro cytopathicity or NSI/SI phenotype with changes in pathogenicity. In light of those studies, it is possible that the cumulative effects of each viral determinant on replication, cytopathicity, and SI capacity may be important for enhancing the pathogenicity of SIVMne.

ACKNOWLEDGMENTS

We thank Mary Poss for critical review of the manuscript. The CEMx174 cell line and GCT-conditioned medium were obtained from the AIDS Research Reagent and Reference Program.

This work was supported by NIH grant RO1 AI34251. J.T.K. was supported in part by NIH training grants T32 CA09229 and T32 AI07140 and an NRSA individual postdoctoral fellowship (F32 AI09337). J.O. is a scholar of the Leukemia Society.

REFERENCES

1. **Benveniste, R. E., R. W. Hill, L. J. Eron, U. M. Csaikl, W. B. Knott, L. E. Henderson, R. C. Sowder, K. Nagashima, and M. A. Gonda.** 1990. Characterization of clones of HIV-1 infected HuT 78 cells defective in gag gene processing and of SIV clones producing large amounts of envelope glycoprotein. J. Med. Primatol. **19:**351–366.
2. **Bosch, M. L., P. L. Earl, K. Fargnoli, S. Picciafuoco, F. Giombini, F. Wong-Staal, and G. Franchini.** 1989. Identification of the fusion peptide of primate immunodeficiency viruses. Science **244:**694–697.
3. **Cao, J., I.-W. Park, A. Cooper, and J. Sodroski.** 1996. Molecular determinants of acute single-cell lysis by human immunodeficiency virus type 1. J. Virol. **70:**1340–1354.
4. **Chackerian, B., L. Rudensey, and J. Overbaugh.** 1997. Specific N-linked and O-linked glycosylation modifications in the envelope V1 domain of simian immunodeficiency virus variants that evolve in the host alter recognition by neutralizing antibodies. J. Virol. **71:**7719–7727.
5. **Chackerian, B., N. L. Haigwood, and J. Overbaugh.** 1995. Characterization of a CD4-expressing macaque cell line that can detect virus after a single replication cycle and can be infected by diverse simian immunodeficiency virus isolates. Virology **213:**386–394.
6. **Cheng-Mayer, C., D. Seto, M. Tateno, and J. A. Levy.** 1988. Biologic features of HIV-1 that correlate with virulence in the host. Science **240:**80–82.
7. **Cheng-Mayer, C., T. Shioda, and J. A. Levy.** 1991. Host range, replicative, and cytopathic properties of human immunodeficiency virus type 1 are determined by very few amino acid changes in *tat* and gp120. J. Virol. **65:**6931–6941.
8. **Chernomordik, L., A. N. Chanturiya, E. Suss-Toby, E. Nora, and J. Zimmerberg.** 1994. An amphipathic peptide from the C-terminal region of the human immunodeficiency virus envelope glycoprotein causes pore formation in membranes. J. Virol. **68:**7115–7123.
9. **Collman, R., J. W. Balliet, S. A. Gregory, H. Friedman, D. L. Kolson, N. Nathanson, and A. Srinivasan.** 1992. An infectious molecular clone of an unusual macrophage-tropic and highly cytopathic strain of human immunodeficiency virus type 1. J. Virol. **66:**7517–7521.
10. **Connor, R. I., and D. D. Ho.** 1994. Human immunodeficiency virus type 1 variants with increased replicative capacity develop during the asymptomatic stage before disease progression. J. Virol. **68:**4400–4408.
11. **Connor, R. I., H. Mohri, Y. Cao, and D. D. Ho.** 1993. Increased viral burden and cytopathicity correlate temporally with $CD4^+$ T-lymphocyte decline and clinical progression in human immunodeficiency virus type 1-infected individuals. J. Virol. **67:**1772–1777.
12. **de Jong, J.-J., J. Goudsmit, W. Keulen, B. Klaver, W. Krone, M. Tersmette, and A. de Ronde.** 1992. Human immunodeficiency virus type 1 clones chimeric for the envelope V3 domain differ in syncytium formation and replication capacity. J. Virol. **66:**757–765.
13. **Dorfman, T., A. Bukovsky, A. Ohagen, S. Hoglund, and H. G. Gottlinger.** 1994. Functional domains of the capsid protein of human immunodeficiency virus type 1. J. Virol. **68:**8180–8187.
14. **Dorfman, T., J. Luban, S. P. Goff, W. A. Haseltine, and H. G. Göttlinger.** 1993. Mapping of functionally important residues of a cysteine-histidine box in the human immunodeficiency virus type 1 nucleocapsid protein. J. Virol. **67:**6159–6169.

15. **Fenyö, E. M., J. Albert, and B. Åsjö.** 1989. Replicative capacity, cytopathic effects and cell tropism of HIV. AIDS **3**(Suppl.)**:**S5–S12.
16. **Fenyö, E. M., L. Morfeldt-Manson, F. Chiodi, B. Lind, A. von Gegerfelt, J. Albert, E. Olausson, and B. Åsjö.** 1988. Distinct replicative and cytopathic characteristics of human immunodeficiency virus isolates. J. Virol. **62:**4414–4419.
17. **Fiore, J. R., A. Bjorndal, K. A. Peipke, M. Di Stefano, G. Angarano, G. Pastore, H. Gaines, E. M. Fenyö, and J. Albert.** 1994. The biological phenotype of HIV-1 is usually retained during and after sexual transmission. Virology **204:**297–303.
18. **Fisher, A. G., L. Ratner, H. Mitsuya, L. M. Marselle, M. E. Harper, S. Broder, R. C. Gallo, and F. Wong-Staal.** 1986. Infectious mutants of HTLV-III with changes in the 3′ region and markedly reduced cytopathic effects. Science **233:**655–659.
19. **Gorelick, R. J., D. J. Chabot, A. Rein, L. E. Henderson, and L. O. Arthur.** 1993. The two zinc fingers in the immunodeficiency virus type 1 nucleocapsid protein are not functionally equivalent. J. Virol. **67:**4027–4036.
20. **Gorelick, R. J., S. M. Nigida, J. W. Bess, L. O. Arthur, and L. E. Henderson.** 1990. Noninfectious human immunodeficiency virus type 1 mutants deficient in genomic RNA. J. Virol. **64:**3207–3211.
21. **Hirsch, V., D. Adger-Johnson, B. Campbell, S. Goldstein, C. Brown, W. R. Elkins, and D. C. Montefiori.** 1997. A molecularly cloned, pathogenic, neutralization-resistant simian immunodeficiency virus, SIVsmE543-3. J. Virol. **71:**1608–1620.
22. **Hirsch, V. M., P. Edmondson, M. Murphy-Corb, B. Arbeille, P. R. Johnson, and J. I. Mullins.** 1989. SIV adaptation to human cells. Nature **341:**572–573.
23. **Ho, S. N., H. D. Hunt, R. M. Horton, J. K. Pullen, and L. R. Pease.** 1989. Site-directed mutagenesis by overlap extension using the polymerase chain reaction. Gene **77:**51–59.
24. **Johnston, P. B., J. W. Dubay, and E. Hunter.** 1993. Truncations of the simian immunodeficiency virus transmembrane protein confer expanded virus host range by removing a block to virus entry into cells. J. Virol. **67:**3077–3086.
25. **Karlsson, A., K. Parsmyr, E. Sandström, E. M. Fenyö, and J. Albert.** 1994. MT-2 cell tropism as prognostic marker for disease progression in human immunodeficiency virus type 1 infection. J. Clin. Microbiol. **32:**364–370.
26. **Kimata, J. T., A. Mozaffarian, and J. Overbaugh.** A lymph node-derived cytopathic simian immunodeficiency virus Mne variant replicates in non-stimulated peripheral blood mononuclear cells. Submitted for publication.
27. **Kodama, T., D. P. Wooley, Y. M. Naidu, H. W. Kestler III, M. D. Daniel, Y. Li, and R. C. Desrosiers.** 1989. Significance of premature stop codons in *env* of simian immunodeficiency virus. J. Virol. **63:**4709–4714.
28. **Koot, M., A. H. V. Vos, R. P. M. Keet, R. E. Y. de Goede, M. Wouter Dercksen, F. G. Terpstra, R. A. Coutinho, F. Miedema, and M. Tersmette.** 1992. HIV-1 biological phenotype in long-term infected individuals evaluated with an MT-2 cocultivation assay. AIDS **6:**49–54.
29. **Lee, S., W. Hu, A. G. Fisher, D. J. Looney, V. F. Kao, H. Mitsuya, L. Ratner, and F. Wong-Staal.** 1989. Role of the carboxy-terminal portion of the HIV-1 transmembrane protein in viral transmission and cytopathogenicity. AIDS Res. Hum. Retroviruses **5:**441–449.
30. **Levy, J. A.** 1993. Pathogenesis of human immunodeficiency virus infection. Microbiol. Rev. **57:**183–289.
31. **Marthas, M. L., R. A. Ramos, B. L. Lohman, K. K. A. Van Rompay, R. E. Unger, C. J. Miller, B. Banapour, N. C. Pedersen, and P. A. Luciw.** 1993. Viral determinants of simian immunodeficiency virus (SIV) virulence in rhesus macaques assessed by using attenuated and pathogenic molecular clones of SIVmac. J. Virol. **67:**6047–6055.
32. **Miedema, F., L. Meyaard, M. Koot, M. R. Klein, M. T. L. Roos, M. Groenink, R. A. M. Fouchier, A. B. Van't Wout, M. Tersmette, P. T. A. Schellekens, and H. Schuitemaker.** 1994. Changing virus-host interactions in the course of HIV-1 infection. Immunol. Rev. **140:**35–72.
33. **Miller, M. A., M. W. Cloyd, J. Liebmann, C. R. Rinaldo, K. R. Islam, S. Z. S. Wang, T. A. Mietzner, and R. C. Montelaro.** 1993. Alterations in cell membrane permeability by the lentivirus lytic peptide (LLP-1) of HIV-1 transmembrane protein. Virology **196:**89–100.
34. **Miller, M. A., R. F. Garry, J. M. Jaynes, and R. C. Montelaro.** 1991. A structural correlation between lentiviral transmembrane proteins and natural cytolytic peptides. AIDS Res. Hum. Retroviruses **7:**511–519.
35. **Miller, M. A., T. A. Mietzner, M. W. Cloyd, W. G. Robey, and R. C. Montelaro.** 1993. Identification of a calmodulin binding and inhibitory peptide domain in the HIV-1 transmembrane glycoprotein. AIDS Res. Hum. Retroviruses **9:**1057–1066.
36. **Morton, W. R., R. E. Benveniste, E. A. Clark, C.-C. Tsai, M. J. Gale, M. E. Thouless, J. Overbaugh, and M. G. Katze.** 1989. Transmission of the simian immunodeficiency virus SIVmne in macaques and baboons. J. Med. Primatol. **18:**237–245.
37. **Myers, G., B. H. Hahn, J. W. Mellors, L. E. Henderson, B. Korber, K. T. Jeang, F. E. McCutchan, and G. N. Pavlakis (ed.).** 1995. Human retroviruses and AIDS. Theoretical Biology and Biophysics Group, Los Alamos National Laboratory, Los Alamos, N.Mex.
38. **Novembre, F. J., P. R. Johnson, M. G. Lewis, D. C. Anderson, S. Klump, H. M. McClure, and V. M. Hirsch.** 1993. Multiple viral determinants contribute to pathogenicity of the acutely lethal simian immunodeficiency virus SIVsmmPBj variant. J. Virol. **67:**2466–2474.
39. **Ottmann, M., C. Gabus, and J. Darlix.** 1995. The central globular domain of the nucleocapsid protein of human immunodeficiency virus type 1 is critical for virion structure and infectivity. J. Virol. **69:**1778–1784.
40. **Overbaugh, J., and L. M. Rudensey.** 1992. Alterations in potential sites for glycosylation predominate during evolution of the simian immunodeficiency virus envelope gene in macaques. J. Virol. **66:**5937–5948.
41. **Overbaugh, J., L. M. Rudensey, M. D. Papenhausen, R. E. Benveniste, and W. R. Morton.** 1991. Variation in simian immunodeficiency virus *env* is confined to V1 and V4 during progression to simian AIDS. J. Virol. **65:**7025–7031.
42. **Ritter, G. D., Jr., M. J. Mulligan, S. L. Lydy, and R. W. Compans.** 1993. Cell fusion activity of the simian immunodeficiency virus envelope protein is modulated by the intracytoplasmic domain. Virology **197:**255–264.
43. **Rudensey, L. M., J. T. Kimata, R. E. Benveniste, and J. Overbaugh.** 1995. Progression to AIDS in macaques is associated with changes in the replication, tropism, and cytopathic properties of the simian immunodeficiency virus variant population. Virology **207:**528–542.
44. **Rudensey, L. M., J. T. Kimata, E. M. Long, B. Chackerian, and J. Overbaugh.** Changes in the extracellular envelope glycoprotein of variants that evolve during the course of SIVMne infection affect neutralizing antibody recognition, syncytia formation and macrophage tropism, but not replication, cytopathicity or CCR-5 coreceptor recognition. Submitted for publication.
45. **Rudensey, L. M., M. D. Papenhausen, and J. Overbaugh.** 1993. Replication and persistence of simian immunodeficiency virus variants after passage in macaque lymphocytes and established human cell lines. J. Virol. **67:**1727–1733.
46. **Schuitemaker, H., M. Koot, N. A. Kootstra, M. W. Dercksen, R. E. Y. de Goede, R. P. van Steenwijk, J. M. A. Lange, J. K. M. E. Schattenkerk, F. Miedema, and M. Tersmette.** 1992. Biological phenotype of human immunodeficiency virus type 1 clones at different stages of infection: progression of disease is associated with a shift from monocytotropic to T-cell-tropic virus populations. J. Virol. **66:**1354–1360.
47. **Slade, A., S. Jones, N. Almond, and P. Kitchin.** 1993. Simian immunodeficiency virus (mac 251-32H) transmembrane protein sequence remains conserved throughout the course of infection in macaques. AIDS Res. Hum. Retroviruses **9:**133–139.
48. **Spies, C. P., G. D. Ritter, Jr., M. J. Mulligan, and R. W. Compans.** 1994. Truncation of the cytoplasmic domain of the simian immunodeficiency virus envelope glycoprotein alters the conformation of the external domain. J. Virol. **68:**585–591.
49. **Srinivas, S. K., R. V. Srinivas, G. M. Anantharamaiah, R. W. Compans, and J. P. Segrest.** 1993. Cytosolic domain of the HIV envelope glycoprotein binds to CaM and inhibits CaM-regulated proteins. J. Biol. Chem. **268:**22895–22899.
50. **Tencza, S. B., T. A. Mietzner, and R. C. Montelaro.** 1997. Calmodulin-binding function of LLP segments from the HIV type 1 transmembrane protein is conserved among natural sequence variants. AIDS Res. Hum. Retroviruses **13:**263–269.
51. **Tersmette, M., R. A. Gruters, F. De Wolf, R. E. Y. De Goede, J. M. A. Lange, P. T. A. Schellekens, J. Goudsmit, H. G. Huisman, and F. Miedema.** 1989. Evidence for a role of virulent human immunodeficiency virus (HIV) variants in the pathogenesis of acquired immunodeficiency syndrome: studies on sequential HIV isolates. J. Virol. **63:**2118–2125.
52. **Tersmette, M., J. M. A. Lange, R. E. Y. DeGoede, F. DeWolf, J. K. M. Eeftink-Schattenkerk, P. T. A. Schellekens, R. A. Coutinho, J. G. Huisman, J. Goudsmit, and F. Miedema.** 1989. Association between biological properties of human immunodeficiency virus variants and risk for AIDS and AIDS mortality. Lancet **i:**983–985.
53. **Valentin, A., J. Albert, E. M. Fenyo, and B. Asjo.** 1994. Dual tropism for macrophages and lymphocytes is a common feature of primary human immunodeficiency virus type 1 and 2 isolates. J. Virol. **68:**6684–6689.
54. **Yang, C., C. P. Spies, and R. W. Compans.** 1995. The human and simian immunodeficiency virus envelope glycoprotein transmembrane subunits are palmitoylated. Proc. Natl. Acad. Sci. USA **92:**9871–9875.
55. **You, J. C., and C. S. McHenry.** 1994. Human immunodeficiency virus nucleocapsid protein accelerates strand transfer of the terminally redundant sequences involved in reverse transcription. J. Biol. Chem. **269:**31491–31495.
56. **Yu, X., M. F. McLane, L. Ratner, W. O'Brien, R. Collman, M. Essex, and T.-H. Lee.** 1994. Killing of primary $CD4^+$ T cells by non-syncytium-inducing macrophage-tropic human immunodeficiency virus type 1. Proc. Natl. Acad. Sci. USA **91:**10237–10241.
57. **Zhang, H., G. Dornadula, P. Alur, M. A. Laughlin, and R. J. Pomerantz.** 1996. Amphipathic domains in the C terminus of the transmembrane protein (gp41) permeabilize HIV-1 virions: a molecular mechanism underlying natural endogenous reverse transcription. Proc. Natl. Acad. Sci. USA **93:**12519–12524.
58. **Zingler, K., and D. R. Littman.** 1993. Truncation of the cytoplasmic domain of the simian immunodeficiency virus envelope glycoprotein increases Env incorporation into particles and fusogenicity and infectivity. J. Virol. **67:**2824–2831.